Iranian Polymer Journal
18 (9), 2009, 703-712

Available online at: http://journal.ippi.ac.ir

Organic Montmorillonite Modified Polyacrylate Nanocomposite by Emulsion Polymerization

Liying Wu, Ming Wang, Xixiang Zhang, Deben Chen, and Anyong Zhong*

College of Chemistry, Sichuan University, Chengdu 610064, PR China

Received 21 January 2009; accepted 5 July 2009

ABSTRACT

A polyacrylate/organic montmorillonite (OMMT) nanocomposite was synthesized by in-situ emulsion polymerization with intercalated structure as demonstrated by X-ray diffractometry. The emulsions and the films obtained from the emulsions prepared were characterized with rotary viscometer, laser light scattering, transmission electron micrograph, scanning electron micrograph, differential scanning calorimetry, the 180ºC peeling intensity test, etc. The results indicated that addition of OMMT improved the engineering properties of emulsions. Among the samples tested, the modified polyacrylate emulsion which was prepared by intercalating 2 wt% OMMT and pretreated with immersion disposal showed the most desirable effect and obtained the following advantages: smaller particle size, stronger pseudo-plastic, better thermal stability, and better adhesion property. The morphology of emulsion particles became a polygon from approximate sphericity. It was also demonstrated by SEM that OMMT addition improved the ductility of the polyacrylate film. Furthermore, the peeling strength was likewise improved with the increased amount of OMMT.

Key Words:

polyacrylate emulsion;
organic montmorillonite;
the particle morphology;
rheology;
the fracture surface morphology.

(*) To whom correspondence to be addressed.
E-mail: zhongany@sina.com.cn

INTRODUCTION

Since the Toyota research group reported the first example of commercialized nanocomposites involving montmorillonite clay in nylon 6 in 1993 [1], polymer/clay nanocomposites have attracted great interest in both industrial and academic laboratories because of the improvements in many physical properties [1-5], including mechanical properties, thermal properties, barrier characteristics, etc. Clay, such as montmorillonite (MMT) with layered silicate, is of special interest because it offers a high aspect ratio (or extremely large surface area) and it is hydrophilic in nature [5,6], so, it is rendered hydrophobic by exchanging the interlayer inorganic cations (Na^+, Ca^{2+}) with organic cation in order to improve the compatibility of the hydrophilic clay and hydrophobic polymer.

Acrylic polymer emulsion with good film-forming property, resistance to chemicals and water, and environmental friendly chemistry

has been widely used in leather coatings, adhesives, and other applications [7]. However, some drawbacks of acrylic emulsion inhibit the extensive application in coatings and adhesives. With the development of polymer/clay composites, MMT is also utilized to improve the properties of polyacrylate nanocomposite. Four methods have been reported in the preparation of this kind of nanocomposite [3,4]: solution intercalation, in situ intercalative polymerization, melt intercalation, and template synthesis.

Under the volatile organic compounds (VOC) regulations strengthened from the viewpoint of environmental protection, considering lower cost, ease of polymerization, in situ emulsion polymerization is the best suited alternative for the production of waterborne nanocomposites for coating and adhesive applications. For instance, Diaconu et al. [4] reported that the waterborne polymer clay nanocomposites (WPCN) were prepared by emulsion and miniemulsion copolymerization of butyl acrylate and methyl methacrylate. Yang et al. [6] prepared acrylic emulsion pressure-sensitive adhesives (PSAS) reinforced with layered silicate by emulsion polymerization. Usually, polymer/clay nanocomposites were produced through waterborne emulsion polymerization using hydrophilic clay or miniemulsion polymerization to facilitate the exfoliation and dispersion of clay, and resulting in large size latex particles [8-11]. Inspired by the Pickering emulsion polymerization [12-14], both emulsifier and organically modified montmorillonite were used to stabilize the emulsion to obtain smaller colloid particles and higher performance polymer/clay composite.

In this paper, polyacrylate/organic montmorillonite nanocomposite emulsions were synthesized by emulsion polymerization. The major concern of this work is to study the effects of the OMMT on the latex particles morphology, rheological property of the emulsion and the fracture surface morphology of latex film. At the same time, the influence of OMMT on the thermal property and peeling strength of polyacrylate/OMMT nanocomposites are also investigated. The results obtained will be helpful for studying the polymer structure, morphology and their inter-relationship with properties.

EXPERIMENTAL

Materials

Sodium montmorillonite (MMT) was supplied by Zhejiang Geologic Institute, and its size is ~100 mesh, and cetyltrimethylammonium bromide (CTAB) was supplied by Shandong Jining Chemical and Technological Institute, China. Sodium silicate (Na_2SiO_3), methyl methacrylate (MMA), butyl acrylate (BA), and acrylic acid (AA) (Beijing East Chemical Industry Factory, China), polyoxyethylated octylphenol (OP-10) (Henkel International, German) were all of industrial grades. Ammonium persulphate (APS), sodium dodecylsulphate (SDS), and ammonium hydroxide ($NH_3.H_2O$) were obtained from AR, Beijing Chemical Plant, China. Sodium hydrogen carbonate ($NaHCO_3$) (AR, Chengdu Kelong Chemical Industry Factory, China). All chemicals were used as received. Deionized water was used throughout the experimental work.

Preparations

Organic montmorillonite was prepared according to workup procedure of reference 15 and the emulsions were prepared by seed emulsion polymerization.

Preparation of the Core-emulsion

A four-necked flask equipped with a stirrer, a condenser and a centigrade thermometer was immersed in a water bath with temperature carefully raised to 74±1ºC. Upon reaching the reaction temperature, the monomers (45 mL BA, 10.7 mL MMA, 1 mL AA), OMMT (various), emulsifiers (2.3 g OP-10 and 1.15 g SDS), sodium hydrogen carbonate (0.105 g), 75 mL H_2O were added into the reaction vessel, the mixture was stirred at the rate of 600 rpm for about 10 min. Then, initiation solution (0.8 g APS in 8 mL H_2O) was introduced to the reaction vessel, the blend was approximately reacted for 1 h. Here a slight blue-colour appeared in the reaction system, this process provided the core-emulsion.

Preparation of the Shell-emulsion

When the core-emulsion was prepared successfully, the second phase of the emulsifier (0.76 g OP-10 and 0.38 g SDS in 50 mL H_2O) and initiator solution APS

Table 1. Data for seeded-emulsion polymerization.

Sample	K	n	η_0 (mPa.s)	OMMT content
A	0.168	0.62	36.3	2.0 wt%
A1	0.097	0.68	28.3	1.5 wt%
A2	0.092	0.67	26.7	1.0 wt%
B	0.493	0.50	106.7	2.0 wt%
C	0.263	0.58	65.0	2.0 wt%
D	0.024	0.90	15.9	0.0 wt%

(4 mL), and mixed monomer (45 mL BA, 10.7 mL MMA, 1 mL AA) was fed continuously to the reaction system in two separate streams for 3 h and the reaction temperature was still maintained at 74±1ºC. Then, the system was heated up to 81±1ºC and maintained at this temperature for 1 h and finally neutralized with aqueous ammonium. Finally, a kind of semi-translucent and blue fluid emulsion with 43~44% solid content was obtained.

In order to investigate the effect of OMMT, a polyacrylate emulsion without adding OMMT was prepared under similar conditions. Table 1 shows different samples procedure data obtained in our laboratory.

Characterization and Testing of Emulsion and Films

X-Ray diffraction (XRD) analysis was performed on a Japan D/max-rA X-ray diffractometer; (Cu-Ka radiation, λ = 0.154 nm, 40 kV, 70 mA). The (001) basal spacing (d) of the MMT was calculated using the Bragg equation [16]:

$$n\lambda = 2d\sin\theta \quad (1)$$

The particle size and particle size distribution (PSD) of emulsions were measured using a laser light scattering (Master Sizer-2000 of Malvern instruments of Worcester, UK).

A rotational viscometer (NXS-IIA, Chengdu Instruments Co., China) was employed to measure the viscosity of emulsions at different shear rates at 25±0.1ºC after the solid content of each emulsion sample was adjusted using distilled water to be equalized.

The size and morphology of the prepared emulsion particles were characterized on a transmission electron microscope (TEM, JEM-100CX, Japan) using 2% aqueous phosphorotungstic acid as a staining agent.

The morphology of the fractured surfaces of the latex films was investigated with Hitachi S-450 scanning electron microscope (SEM). SEM was operated at 75 kV. The specimens were frozen under liquid nitrogen, then fractured, mounted, and coated with gold (300A) on Edwards S 150B sputter coater.

A NETZSCH DSC differential scanning calorimeter (200 PC, GER) was used to test the glass transition temperature and thermal decomposition temperature of the latex films.

The 180ºC peel intensity test was adopted according to the national standard method of (GB 2791-81), China. Peeling intensity was performed by an electronic universal testing machine XLW-100N (China; 180º peeling angle).

RESULTS AND DISCUSSION

The XRD Patterns of Polyacrylate/OMMT Nanocomposites, Na-MMT and OMMT

Figure 1 shows a series of XRD patterns of films prepared with samples A, B, and C together with Na-MMT and OMMT. Pristine Na-MMT shows a characteristic diffraction peak at 7.94º, corresponding

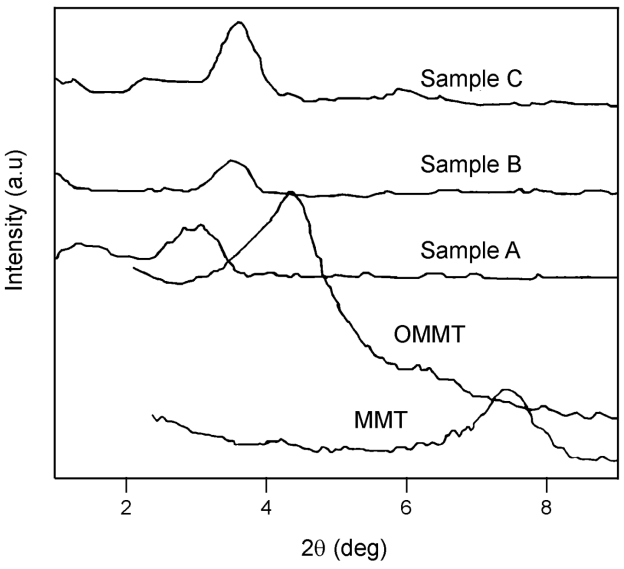

Figure 1. X-Ray diffcation patterns for MMT, OMMT, and for samples obtained from different disposal methods of 2 wt% OMMT.

to the d-spacing of 1.15 nm on Bragg equation. For OMMT, the diffraction peak is observed at 4.46º corresponding to the d-spacing of 1.94 nm. The results show that organic CTAB has been intercalated between MMT layers. Besides, the diffraction peak of samples A, B, and C were around 3~3.4º, corresponding to the d-spacing of 2.94 to 2.60 nm indicating further enlarged interlayer space. This increase could probably originate from the intercalation of polymeric molecules within the galleries of the hydrophilic silicate. Furthermore, when organophilic MMT is added to the system, an exfoliated morphology might be obtained.

The Particle Size and Particle Distribution of the Emulsion

The particle size and PSD of samples A, B, C, and D are shown in Figure 2. The geometric mean diameter (d_g) is calculated according to eqn (2) [17].

$$d_g = \exp[\sum (n_i \ln d_i) / N] \quad (2)$$

where n_i is the number of particles in group i, with a midpoint of size d_i, and $N = \Sigma n_i$, means the total number of particles.

Particle size distribution breadth (B) was calculated according to eqn (3) [18].

$$B = (D_{90} - D_{10}) / D_{50} \quad (3)$$

where D_{90}, D_{50}, and D_{10} are the particle diameters for the 90th, 50th, and 10th cumulative mass percentiles, respectively.

According to Figure 2 and eqns (2) and (3), the average size and PSD of latex particles take place a great change as the result of OMMT presence. The average particle diameters of the emulsions are 63.4 nm, 61.4 nm, 78.1 nm, and 80.5 nm, from left to right, respectively, with all under 100 nm, the corresponding particle size distributions are 1.30, 1.29, 1.30, and 0.71, respectively. These results indicate that the polyacrylate/OMMT emulsions exhibit smaller average particle size and wider particle distribution compared to the polyacrylate emulsion.

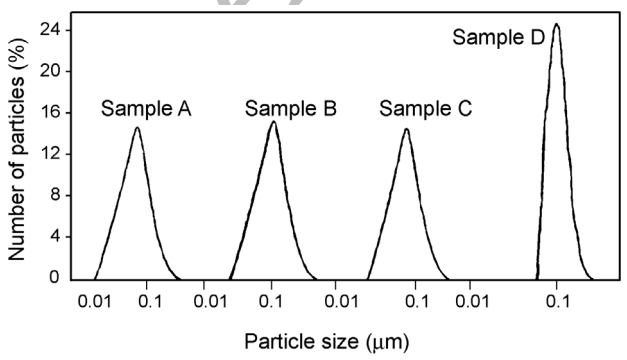

Figure 2. Laser light scattering graphs of latexes.

The TEM Experiment

In order to study the effects of OMMT on the prepared polyacrylate emulsion, TEM was used to make comparative study between the latex particle size and morphology of the samples A, B, C, and D.

Figure 3 shows the TEM photographs of polyacrylate emulsion with and without the presence of 2 wt% OMMT. From the TEM photograph above, the particle morphology of the polyacrylate emulsion exhibited a great change with the presence of OMMT. In this figure, the latex particles morphology of the sample D was sphericity, while the sample B produced a small deformation in terms of the latex particles morphology. However, the latex particles of the samples A and C showed a clear polygon-like. Furthermore, the particle size of pure polyacrylate emulsion was bigger and had a narrower distribution compared to that of the PA/OMMT emulsions. This phenomenon is consistent with the results from the laser light scattering for the emulsions.

In this system, CTAB-modified montmorillonite platelets in size of several hundreds of nanometers tend to disperse within monomer droplets in scale of micrometer, although there are numerous micelles or monomer-swollen micelles in smaller size in the emulsion system. So, it is not difficult to understand that the polymerization takes place in the monomer-swollen micelles instead of clay containing monomer droplets. However, along with the growth of latex particles, more monomers in droplets diffuse into the latex particles through water phase, and monomer droplets become smaller and smaller in size and finally disappear. Then the OMMT is forced to enter into the water phase. But this state is not stable, and the hydrophobic surface of OMMT platelets makes them bind to the surface of latex particles, instead of

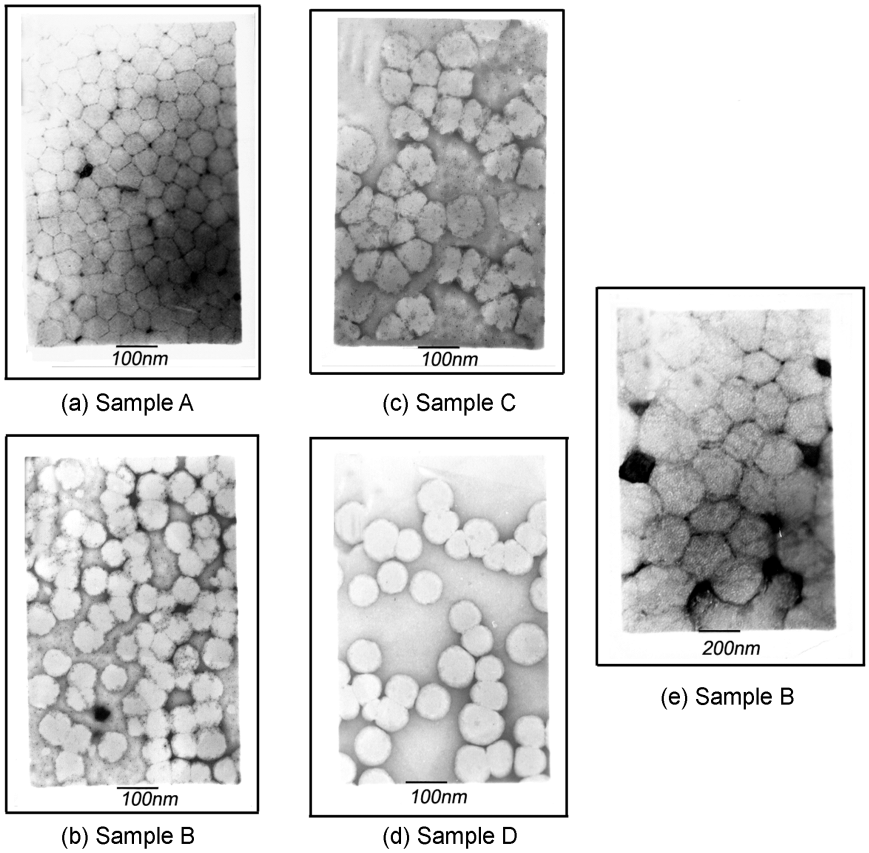

Figure 3. TEM micrographs of the particle morphology of the polyacrylate emulsions: (a), (c) samples obtained from different disposal methods of 2 wt% OMMT, (b) and (e) sample B, (d) sample without OMMT (magnification: (a)-(d) 50 k, (e) 100 k).

diffusing into latex particles due to the mismatch between OMMT platelets and latex particles in size. Similar to the Pickering emulsion mechanism [12-14], the clays on the surface of latex particles prevent the particles from coalescing, especially, better exfoliation of montmorillonite platelets will result in more stable emulsion and smaller particles, which was verified in Figure 3, herein sample A had smaller particles than others with or without clay. Because of a faceting effect caused by the rigidity of the clay platelets, the colloid particles are not perfectly spherical [19], as shown in Figures 3a, 3b, and 3c. It is also observed in Figure 3 that the colloid particles are not isolated but tend to assemble together. This can be explained by the fact that in this system, organically modified clay has effective stabilization for colloid particles and two colloid particles share the same clay layer [19]. Figure 3e shows the morphology of sample B with a magnification of 100000. It can be clearly seen that most clays exist outside colloid particles, preferentially on the surface of colloid particles. In short, the morphology and distribution of clay in this system is sophisticated and further study will be conducted in the future.

Rheological Behaviour of the Emulsion

Rheological property is a key factor for an emulsion. The rheological properties of prepared samples were examined with the same emulsifier and solid content at 25ºC. The plots of the apparent viscosity (η_a) versus the shear rate (γ) are given in Figure 4.

From the curves in Figures 4a and 4b, the apparent viscosity (η_a) decreased with increasing shear rate. The typical shear thinning behaviour of pseudo-plastic liquid is shown, which is explained according to the Mooney equation [20]:

$$\ln \eta_\alpha = \ln \eta_e + K_e V_i / (1 - V_i / \varphi) \quad (4)$$

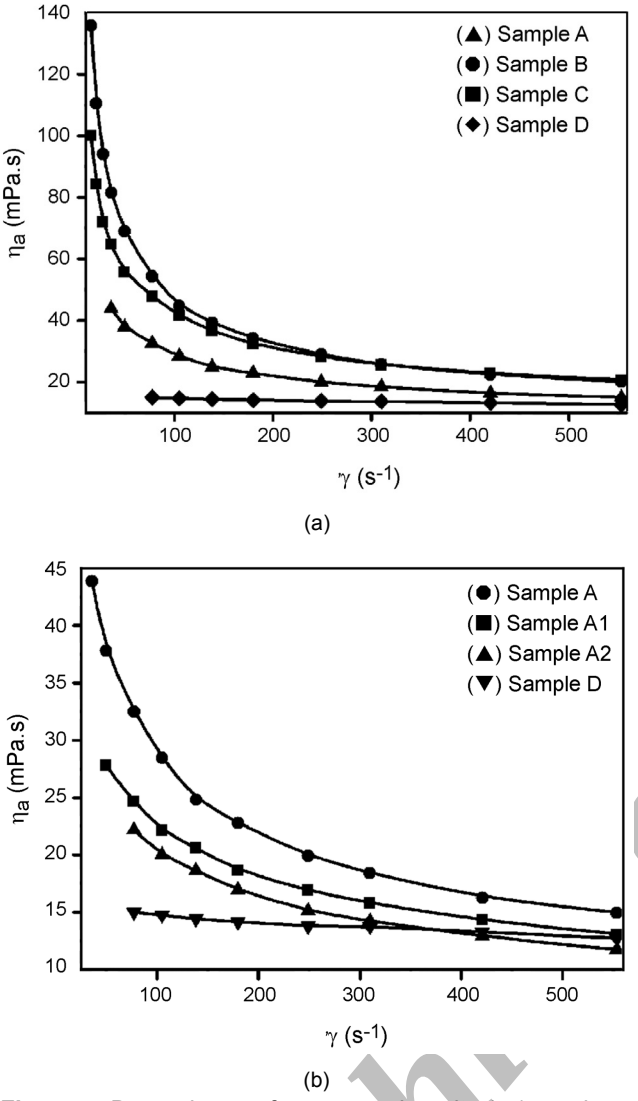

Figure 4. Dependence of apparent viscosity (η_a) on shear rate (γ) of emulsions. Rheological behaviour curves of: (a) different disposal methods of OMMT and (b) different OMMT content.

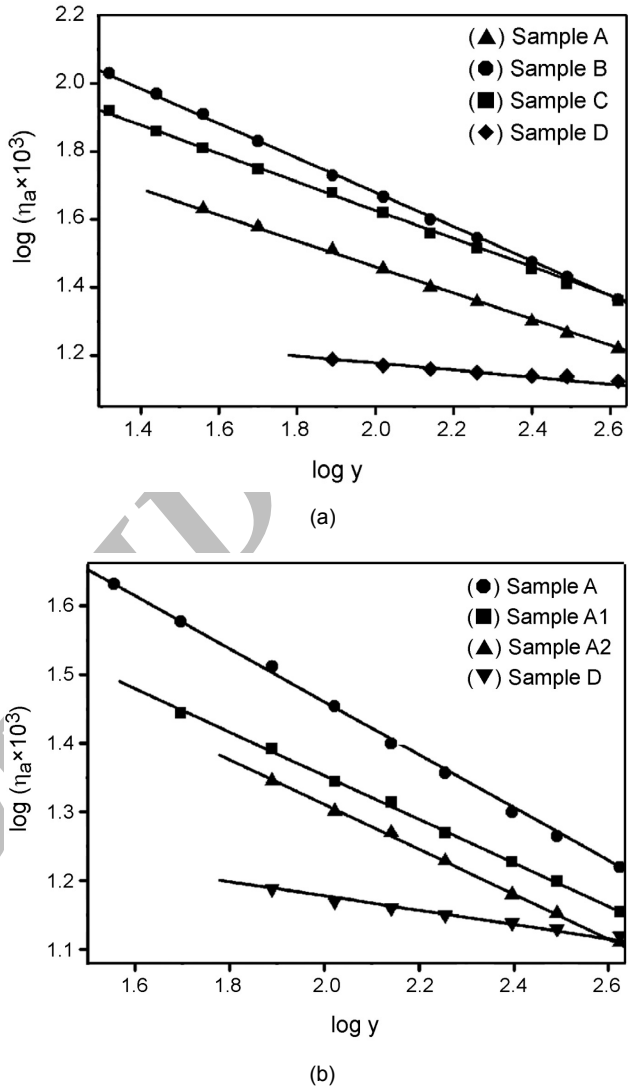

Figure 5. Dependence of log ($\eta_a \times 10^3$) versus log γ: (a) different disposal methods of OMMT and (b) different OMMT content.

where η_α is the apparent viscosity, K_e is form constant of particle, η_e is the viscosity of the continuous phase, V_i is volume fraction of dispersed phase, and φ is packed coefficient. The latex particles were distorted and deformation occurred at shear action. The K_e value decreased and φ value increased after the emulsion was sheared, which caused a decrease in η_α. Besides, this phenomenon can also explain the shear-induced orientation effect. Shear-induced orientation can lead to a considerable decrease in the sample viscosity. Krishnamoorti et al. reported that even at the lowest shear rates accessed in the steady shear measurements for the PS-PI/clay nanocomposites, significant orientation of the layered silicate occurs [21].

The rheological property of emulsion was analyzed in linear regress equation to know the relationship among the different OMMT contents, different pretreatment methods for OMMT, and the rheological behaviour. According to Oswald-de Waele power-law equation: $\eta_a = K\gamma^{n-1}$ [22], it can be obtained that:

$$\log \eta_a = \log K + (n-1)\log \gamma \quad (5)$$

where K is consistency factor, which is proportional to the apparent viscosity, n is the flow index; $n < 1$, to

Table 2. Values of consistency factor (K), flow index (n), and zero shear viscosity (η_0) of emulsion.

Sample	OMMT content	OMMT and core-monomer disposal method
A, A1, A2	2 wt%, 1.5 wt%, 1 wt%	OMMT was dipped in the core-monomer for 24 h before polymerization
B	2 wt%	OMMT and core-monomer were sonicated in water bath for 15 min at room temperature before polymerization
C	2 wt%	No treatment for OMMT before polymerization
D	0 wt%	Without OMMT

non-Newtonian fluid, n = 1, to Newtonian fluid. The values of K and n of polyacrylate emulsion can be obtained from the linear relationship log η_α and log γ in Figure 5 and are listed in Table 2.

From Figure 5 and Table 2 it is evident that the values of K are increased with increasing the content of OMMT, while the values of n are inversely proportional to the OMMT content and all being smaller than 1. The results again prove all the polyacrylate/OMMT emulsions to be a stronger pseudo-plastic fluid. Comparing the three samples with the same OMMT content of 2 wt%, the parameter K of the sample A, synthesized with 2 wt% OMMT and pretreating with immersion disposal, is the smallest. However, the corresponding value of n is the biggest. The possible reason is discussed as follows:

When shear rate (γ) is zero, zero shear viscosity can be obtained from Cross equation [23]:

$$1/\eta_a = 1/\eta_0 + (a/\eta_0)\cdot\gamma^{2/3} \quad (6)$$

where η_0 is the zero shear viscosity, η_0 is calculated by eqn (6) and it is shown in Table 2.

From Table 2, η_0 of emulsion was increased with the increased content of OMMT, meanwhile, η_0 value of the sample A turns out to be the smallest among the polyacrylate emulsions containing 2 wt% of OMMT. These results may be related to the polymer chains hindrance by clay platelets and the clay platelet dispersion in a polymer matrix. Generally speaking, when the silicate layers are uniformly dispersed in the polymer matrix, the emulsion will flow easily under low shear rates and shear force. On the contrary, if the silicate layers are not well dispersed in the system, tactoids and aggregates of clay platelets will hinder the emulsion flow, which means that greater shear force should be applied in the shear process. Besides, more tactoids and aggregates of clay platelets will occur in the emulsion system with increasing the clay loading. So, it is not difficult to understand that why the apparent viscosity and zero shear viscosity should increase with the content of OMMT, and that of sample A with 2 wt% OMMT pretreating with immersion disposal are smallest compared to the other emulsions containing 2 wt% of OMMT.

On the other hand, clay sheets are highly anisotropic inorganic nanoparticles, which can be oriented under shear field. The silicate layers are randomly organized under quiescent conditions, and with increasing shear force, the silicate layers gradually orient themselves with the layers aligned parallel to the flow direction. At high shear rate, the viscosity of emulsion containing OMMT is comparable to that of the pure polyacrylate emulsion. Consequently, the pseudo-plasticity of polyacrylate emulsion is obviously reinforced by adding OMMT. This actually facilitates the painting process with less painting back and forth.

The SEM Experiment

In order to study the effects of OMMT on the prepared polyacrylate latex film, SEM is used to comparatively study the fracture morphology of the samples with and without 2 wt% OMMT.

Figure 6 shows the fracture morphology of the samples C and D. Herein, sample D displays order stripes and sample C presents the disorder stripes in the same figure. It is clearly indicated that the pure polyacrylate film exhibits smooth brittle fracture surface, while the polyacrylate film with 2 wt% OMMT shows the characteristics of ductile fracture.

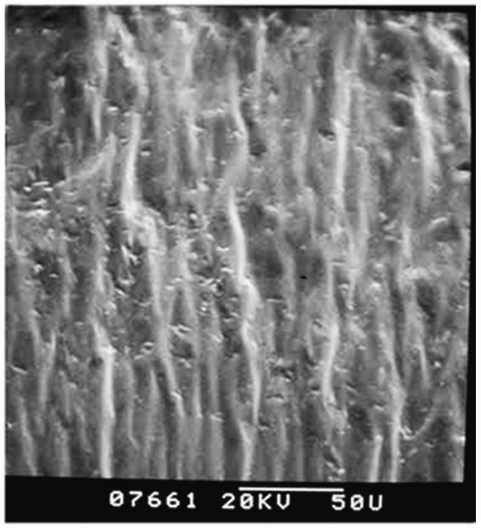

(a) Sample C

(b) Sample D

Figure 6. The fraction surface morphology of the polyacrylate films: (a) 2 wt% OMMT and (b) 0 wt% OMMT.

The above phenomenon indicates that the addition of OMMT can improve the ductility of the polyacrylate film. This is because MMT layers with large aspect ratio have been involved in the polyacrylate matrix which bring along better flexibility [24,25].

Thermal Properties

The DSC analysis is used to investigate thermal decomposition temperature and the glass transition temperature (T_g) for the polyacrylate films with and without OMMT. As it is observed from Table 3, with increased OMMT loading, the thermal stability of the polyacrylate film is increased moderately, though the T_g shows only a slight improvement. When the content of the OMMT is about 2 wt%, the decomposition temperature of the sample B increases by approximately 10ºC and T_g increases around 3°C, compared to the pure polyacrylate film. Furthermore, comparing the three polyacrylate/OMMT nanocomposites with the same amount of OMMT (2 wt%) present, the decomposition temperature and T_g show no significant differences.

The results indicate that MMT as an inorganic material dispersed in the polymer matrix has a high thermal stability itself and retards the heat transmission quickly and limiting the continuous decomposition of the nanocomposite. On the other hand, a slight increment of T_g of polyacrylate/OMMT nanocomposites indicates that the OMMT presence in the polyacrylate matrix does not affect the toughness of polyacrylate film.

The 180°C Peeling Strength

Adhesive tapes were prepared by coating the samples

Table 3. The thermal properties and peeling strength of samples.

Sample	Decomposition temperature (ºC)	Glass transition temperature (ºC)	180°C Peel strength (N/25 mm)	OMMT content
A	406.8	-24.7	2.395	2.0 wt%
A1	405.9	-26.0	1.258	1.5 wt%
A2	403.6	-26.9	1.140	1.0 wt%
B	408.6	-25.9	0.748	2.0 wt%
C	406.0	-25.7	1.428	2.0 wt%
D	397.6	-27.5	1.108	2.0 wt%

onto polypropylene (PP) sheets. The test results are presented in Table 3. It is clear from Table 3 that the peeling strength is improved with the increase of OMMT. This may be derived from the diminution of surfactant enrichment at the surface of polyacrylate film by OMMT [26,27].

Comparing the three polyacrylate/OMMT films containing the same amount of OMMT (2 wt%), sample A shows the highest peeling intensity. However, the peeling strength of sample B is even lower than that of the pure polyacrylate (sample D). The low peeling strength of sample B can be explained that it had poor dispersion of MMT aggregates in the polyacrylate system.

CONCLUSION

The properties of the intercalated polyacrylate/OMMT nanocomposite were prominently improved by in-situ emulsion polymerization. Better engineering properties can be obtained for the polyacrylate/OMMT emulsion synthesized with immersion treatment for OMMT. Compared with the polyacrylate emulsion, this modified emulsion containing 2 wt% OMMT shows the following advantages: smaller particle size, stronger pseudo-plasticity, better thermal stability, and better adhesion property. Moreover the morphology of emulsion particles becomes polygon from approximate sphericity. In addition, SEM images indicate that the addition of OMMT improves the ductility of the polyacrylate film. The peeling strength is improved with the increased OMMT content.

ACKNOWLEDGEMENTS

The authors gratefully acknowledge financial support of the National Nature Science Foundation of China (grant No. 50573050) and SiChuan Provincial Department of Technology in China (2006Z02-03). This work has benefited from the use of instruments analytical-testing centre of Sichuan University, China. The authors are grateful to Dr Y He and HQ Lin for their skillful help with SEM and TEM images, respectively.

SYMBOLS AND ABBREVIATIONS

OMMT	: organic montmorillonite
VOC	: volatile organic compounds
MMA	: methyl methacrylate
BA	: butyl acrylate
AA	: acrylic acid
OP-10	: polyoxyethylated octylphenol
APS	: ammonium persulphate
SDS	: sodium dodecylsulphate
DSC	: differential scanning calorimetry
XRD	: X-ray diffractometry
TEM	: transmission electron micrograph
SEM	: scanning electron micrograph
K	: constant of the instrument
α	: the numerical reading on the instrument
K	: consistency factor
η_a	: apparent viscosity
η_0	: zero shear viscosity
γ	: the shear rate
d_g	: geometric mean diameter
n_i	: number of particles in group i
d_i	: size at midpoint
N	: total number of particles
B	: particle size distribution breadth
D_{90}, D_{50}, D_{10}	: the particle diameters for the 90th, 50th and 10th cumulative mass percentiles, respectively.

REFERENCES

1. Usuki A, Kojima Y, Kawasumi M, Okada A, Fukushima Y, Kurauchi Y, Kamigaito O, Synthesis of nylon 6-clay hybrid, *J Mater Res*, **8**, 1179-1184, 1993.
2. Wang YQ, Zhang HF, Wu YP, Preparation and properties of natural rubber/rectorite nanocomposites, *Eur Polym J*, **41**, 2776-2783, 2005.
3. Barmar M, Barikani M, Fereidounnia M, Study of polyurethane/clay nanocomposites produced via melt intercalation method, *Iran Polym J*, **15**, 709-714, 2006.
4. Diaconu G, Asua JM, Paulis M, Leiza JR, High-solids content waterborne polymer-clay nanocomposites, *Macromol Symp*, **259**, 305-317, 2007.

5. Patel HA, Somani RJ, Bajaj HC, Jasrva RV, Nanoclays for polymer nanocomposites, paints, inks, greases and cosmetics formulations, drug delivery vehicle and waste water treatment, *Bull Mater Sci*, **29**, 133-145. 2006.
6. Li H, Yang YK, Yu YZ, Acrylic emulsion pressure-sensitive adhesives (PSAS) reinforced with layered silicate, *J Adhes Sci Technol*, **18**, 1759-1770, 2004.
7. Liu XH, Zhang CZ, Xiong T, Chen D, Zhong A, Rheological and curing behavior of aqueous ambient self-crosslinkable polyacrylate emulsion, *J Appl Polym Sci*, **106**, 1448-1455, 2007.
8. Sedláková Z, Plestil J, Baldrian J, Slouf M, Holub P, Polymer-clay nanocomposites prepared via in situ emulsion polymerization, *Polym Bull*, **63**, 365-384, 2009.
9. Chern CS, Lin JJ, Lin YL, Lai SZ, Kinetics of styrene emulsion polymerization in the presence of montmorillonite, *Eur Polym J*, **42**, 1033-1042, 2006.
10. Sun QH, Deng YL, Zhong LW, Synthesis and characterization of polystyrene-encapsulated laponite composite via miniemulsion polymerization, *Macromol Mater Eng*, **289**, 288-295, 2004.
11. Moraes RP, Santos AM, Oliveira PC, Souza FCT, Do Amoral M, Volera TS, Demarquette NR, Poly(styrene-*co*-butyl acrylate)-Brazilian montmorillonite nanocomposites, synthesis of hybrid latexes via miniemulsion polymerization, *Macromol Symp*, **245-246**, 106-115, 2006.
12. Pickering SU, Pickering: emulsion, *J Chem Soc*, **91**, 2001-2021, 1907.
13. Velikov KP, Velev OD, Stabilization of thin films, foams, emulsions and bifluid gels with surface-active solid particles, In: *Colloid Stability and Application in Pharmacy*, Tadros TF (Ed), Wiley-VCH, Weinheim, 277-306, 2007.
14. Vroon DJ, Ming W, Van Herk AM, Polymer-clay nanocomposite latex particles by inverse pickering emulsion polymerization stabilized with hydrophobic montomorillonite platelets, *Macromolecules*, **39**, 2137-2143, 2006.
15. Feng XP, Zhong AY, Chen DB, Preparation and properties of poly(silicone-*co*-acrylate)/montmorillonite nanocomposite emulsion, *J Appl Polym Sci*, **106**, 3963-3970, 2006.
16. Sadhu S, Bhowmick AK, Preparation and properties of styrene-butadiene rubber based nanocomposites: the influence of the structural and processing parameters, *J Appl Polym Sci*, **92**, 698-709, 2004.
17. Hinds WC, *Aerosol Technology*, 2nd ed, Wiley, New York, 1999.
18. Lin KJ, Dai CA, Lin KF, Revisit to the formation mechanism of exfoliated montmorillonite/PMMA nanocomposite latex through soap-free emulsion polymerization, *J Polym Sci Part A: Polym Chem*, **47**, 459-466, 2009.
19. Zhang J, Chen KQ, Zhao HY, PMMA colloid particles armored by clay layers with PDMAEMA polymer brushes, *J Appl Polym Sci*, **46**, 2632-2639, 2008.
20. Wicks ZW, Anderson EA, Culhane WJ, Morphology of water-soluble acrylic copolymer solutions, *J Coat Tech*, **54**, 57-61, 1982.
21. Krishnamoorti R, Ren JX, Sliva AS, Shear response of layered silicate nanocomposites, *J Chem Phys*, **114**, 4968-4973, 2001.
22. Liu GJ, *Water Dispersible Coatings*, China Light Industry Press, Beijing, 2004.
23. Han CD, *Rheology in Polymer Processing*, Academic, New York, 1976.
24. Li Y, Zhao B, Xie SB, Zhang SM, Synthesis and properties of poly(methyl methacrylate)/montmorillonite (PMMA/MMT) nanocomposites, *Polym Int*, **52**, 892-898, 2003.
25. Ahmadi SA, Yudong H, Li W, Synthesis of EPDM/organoclay nanocomposites: effect of the clay exfoliation on structure and physical properties, *Iran Polym J*, **13**, 415-422, 2004.
26. Zhao CL, Holl Y, Pith T, Lambla M, Surface analysis and adhesion properties of coalesced latex films, *Brit Polym J*, **21**, 155-160, 1989.
27. Fukuzawa K, *J Adhes Soc Jpn*, **5**, 294-302, 1969 (in Japanese).